Plasma diagnostics and simulations

Spectroscopy of diatomic molecules in plasma

Tasks

1. According to instructions, measure a molecular spectrum in a plasma.
2. Evaluate the measurements.

Why should we care about molecules in plasma?

The internal quantum states of both atoms and molecules serve as reservoirs of energy. When the environment is allowed to reach thermal equilibrium, the population n of quantum states follows Boltzmann distribution

$$n(E) \propto g \cdot \exp\left(-\frac{E}{kT}\right), \tag{1}$$

where E is the amount of energy required to excite the state (i.e. how much energy fits in and can be stored), g is the statistical weight usually called "degeneracy", k is the Boltzmann's constant and T is called temperature. As can be seen, T is a parameter of the distribution function. However, it is not guaranteed that the distribution function can be always described by this parameter. Moreover, the link between a spectroscopically determined temperature and some useful physical parameter of the ambient environment does not need to be straightforward.

In most non-isothermic laboratory discharges, the electric field affects only the charged particles and collisions are the dominant mean of energy redistribution among electrons, ions, atoms and molecules. The presence of electric field distorts the equilibrium and the Boltzmann distribution (8) does not necessarily hold any more. Knowing the deviations from Boltzmann distribution can provide important insight into the energy redistribution pathways in the plasma.

The relative populations of the internal quantum states of the particles in plasma can be determined by spectroscopic methods. In laboratory discharges we often observe emission in the ultraviolet (UV) or visible spectral regions, which is caused by simultaneous transition in electronic, vibrational and rotational state of molecules or electronic states of atoms. These phenomena are studied by optical emission spectroscopy and provide insight into the very energetic electronically excited and readily emitting quantum states. These never stay excited long and are thus rather inefficient energy reservoirs. Still, analysis of optical emission spectra of molecules can give important information also about other species.

There is no general rule how each quantum state is populated as it strongly depends on the particle environment. Mostly we deal with population of quantum states via collisions with other particles. As likelihood of energy transfer is maximal for similar energies we can deduce some basic patterns. For example in most plasmas only the electrons have enough energy to excite particle into upper electronic states (up to 20 eV) so we can assume that the population these states will correlate with energy distribution of electrons. On the other hand the energy for rotational excitations is in order of meV which corresponds to translational energy of molecules of neutral gas so we can assume that distribution of rotational quantum states will correlate to temperature of neutral gas. Sometimes however these assumptions may fail due to the involvement of more complex proces as plasma chemistry etc.

Table 1: List of quantum numbers used in this chapter and their meaning.

symbol	meaning
J	total orbital momentum
N (K in [3])	total orbital momentum apart from the electronic spin
S	orbital momentum of electronic spin

The optical emission spectra of OH can hold information about the energy of electrons [1] (not directly the electron temperature T_e, though) or the chemical pathways that led to the creation of OH molecules [2]. Similarly, nitrogen molecules excited through collisions with argon metastables $\mathrm{Ar}(^3P_2)$ have strongly underpopulated $\mathrm{N_2}(\mathrm{C}\,^3\Pi_u, v' > 2)$ and the spectral bands emitted from these states are missing in the observable spectra.

The population distribution and its deviations from expectations in the low-lying ground electronic states are no less interesting. Here, absorption based methods must often be used, as infra-red spectra are more difficult to acquire. One method accessible in the Department of Physical Electronics is laser-induced fluorescence (LIF). Observing the fluorescence after laser absorption is a powerful alternative to observing just the decrease of laser energy after passing through absorbing medium – the sensitivity may be greatly enhanced by spectral and/or temporal separation of the laser light from the fluorescence. Also, when observing the fluorescence perpendicularly to the laser beam, the probed volume is defined by intersection of the laser light with the line of sight so the probed volume is better defined compared to absorption spectroscopy.

OH radical as an example for nomenclature of molecular quantum states

In this section, we will briefly summarise the structure of the OH radical focusing on how it affects its spectrum. For details, see the comprehensive book of Herzberg [3].

The two most relevant electronic states for OH spectroscopy are the ground state $\mathrm{X}\,^2\Pi$ and the first excited state $\mathrm{A}\,^2\Sigma^+$, in further text we will call them briefly X and A. They are approximately 4 eV apart. This energy gap corresponds to photon wavelengths around 300 nm. Both mentioned electronic states have resulting spin 1/2 and are thus doublets.

The ground electronic state is a Π state, i.e. the resulting length Λ of the projection of the electronic orbital angular momentum to the internuclear axis is 1. For lower rotational states, the dominant fine-structure splitting mechanism is the spin-orbit coupling. However, for higher rotational states the spin-rotational coupling starts to gain importance and for $J \geq 8.5$ starts to dominate. The ground electronic state is thus an intermediate state between Hund's cases (a) and (b). Consequently, neither the J nor the N quantum number is considered "good", but both are "almost good" and can be used to label the rotational states depending on the preference[1]. The relation between the two is $J = N \pm 1/2$ for the fine structure components, usually labelled 1 and 2, respectively. The Λ-doubling effect is also present. Effectively, there are always four different states with the same vibrational and rotational excitation – two orientations of the electronic spin (spin-orbit and spin-rotational splitting) and two orientations of the projection of total orbital momentum of electrons to the internuclear axis. Due to symmetry selection rules (only $+ \leftrightarrow -$ transitions[2] are allowed), only one of the two Λ-doublet components is available for the photon

[1] In this text we adopt the newer notation with J for the quantum number describing the total orbital momentum (apart from the nuclear spin that will be neglected in the whole chapter), N for the total orbital momentum *apart from the electronic spin*, R for pure rotation (seldom used) and S for orbital momentum of electronic spin, as in [4, 5]. In the Herzberg's book, the same quantum numbers are called J, K, N and S, respectively.

[2] $+$ and $-$ denote the so called *parity* of the wavefunction, i.e. action of mirroring the wavefunction with respect to a plane containing the internuclear axis. $+$ denote symmetric wavefunctions, $-$ antisymmetric.

absorption. This is important to take into account when calculating the radical concentration from the LIF measurements.

The first excited state A is a Σ state, i.e. $\Lambda = 0$. Σ electronic states are best described by the Hund's case (b), the good quantum number for rotational state is N. There is no spin-orbit coupling and no Λ-doubling effect. The fine-structure splitting happens solely due to spin-rotational interaction. In this case, the energy spacing of the doublet levels is given by $\gamma\,(N+1/2)$, i.e. increases linearly with rotational quantum number. The energy splitting of the doublet components is smaller compared to the $X\,^2\Pi$ state.

The structure of the OH energy levels is sketched in figure 1. The $A\,^2\Sigma$ state is affected by the spin-rotation interaction which causes a splitting of each rotational state into two sub-levels. Similarly, the $X\,^2\Pi$ state is affected dominantly by the spin-orbit interaction. Each of these two effects causes doubling of each expected rotational line, so we have four lines for $\Delta J = -1$, four lines for $\Delta J = 0$ and four other lines for $\Delta J = +1$ for each rotational level N''. This makes 12 lines altogether. The Λ-doubling of the $^2\Pi$ state, on the other hand, introduces no further splitting of the observed rotational lines. This is because of the $+\leftrightarrow-$ parity selection rule. Because of the Λ-doubling, the $\mathrm{Q}(N'')$ lines have different lower state than $\mathrm{P}(N'')$ or $\mathrm{R}(N'')$ lines. Here, we have used the standard spectroscopic abbreviation: single prime (N') is used to describe the upper state of a transition (here exclusively the electronic state A) and double prime (N'') describes the lower state (here exclusively the X electronic state).

Excitation schema

Although only one specific rotational level can be excited by laser with narrow spectral linewidth, collisional processes can change both vibrational and rotational state of the excited molecular species. As a result, the fluorescence spectrum of OH radicals usually consists of numerous rotational lines that are merged to several vibrational bands. The composition of fluorescence spectrum depends markedly on particular vibrational state that is excited by laser:

1. The simplest situation is realized when OH radicals are excited to the ground vibrational state $A^2\Sigma^+(v' = 0)$ [6]. When no thermal excitation to higher vibrational states occurs, the only intensive fluorescence radiation is the $0-0$ vibrational band located between 306 and 314 nm. Other vibrational bands originating from the ground vibrational state are weak due to their low Franck-Condon factors. Since excitation and fluorescence wavelengths coincide, the fluorescence signal can not be separated from scattered laser radiation spectrally. Consequently, this excitation schema can be used for LIF experiments only when temporal separation can be used, i.e. when the life-time of the excited OH state is longer than the laser pulse duration and the fluorescence signal can be detected after the end of the laser pulse.
2. The spectral separation is simply achieved when OH radicals are excited to the first vibrationally excited state $A^2\Sigma^+(v' = 1)$. In this case, excitation wavelengths around 282 nm are used. Fluorescence vibrational bands $1-1$ ($312-320$ nm) and $0-0$ ($306-314$ nm) are usually used for detection, that can be separated from scattered excitation radiation by spectral filters. The $0-0$ vibrational band arises due to the collisional vibrational energy transfer (VET) and its intensity depends on the ratio between the VET rate and the total deexcitation rate of the $(v' = 1)$ state.
3. Alternatively, higher vibrational states can be excited as well. In these cases the kinetics of excited states is even more complicated. Excitation to the $A^2\Sigma^+(v' = 3)$ state is sometimes used, since this state undergoes rapid predissociation, which reduces the dependence of excitation state life-time on collisional quenching. On the other hand, the dissociation reduces the fluorescence signal and the influence of collisional processes on the life-time of excited OH radicals is not entirely avoided, especially at high pressure. That is why we will further concentrate only on excitation to the $v' = 0$ and $v' = 1$ state.

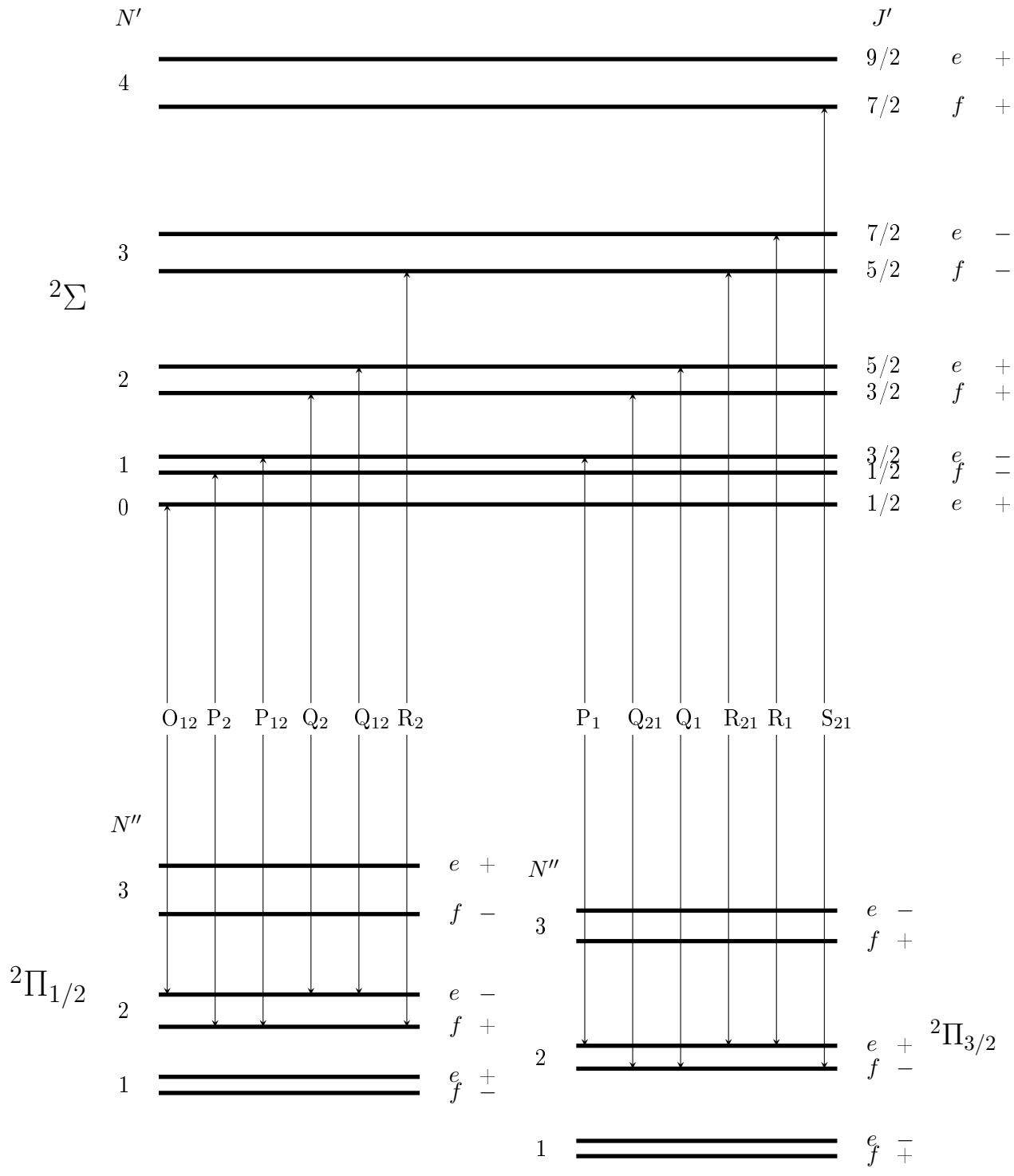

Figure 1: Diagram of $^2\Sigma \leftrightarrow ^2\Pi$ transitions. The J values are omitted for the $^2\Pi$ state. It would be $J = N - 1/2$ for the $^2\Pi_{1/2}$ state and $J = N + 1/2$ for the $^2\Pi_{3/2}$. The lines are labelled according to Hund's case (b), i.e. P for $\Delta N = -1$, Q for $\Delta N = 0$ and R for $\Delta N = 1$.

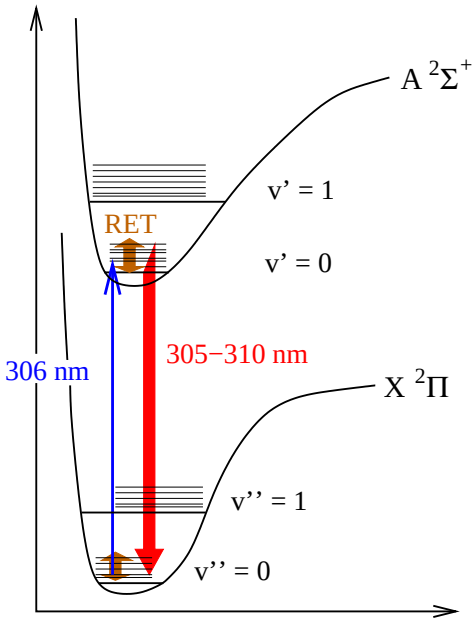

Figure 2: *Fluorescence schema of the excitation to the $v' = 0$ state of OH radicals.*

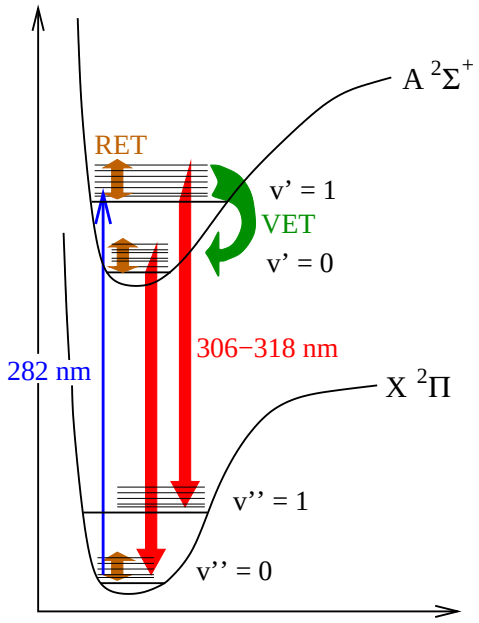

Figure 3: *Fluorescence schema of the excitation to the $v' = 1$ state of OH radicals.*

The vibrational and rotational distribution of the excited state should be taken into account during processing of measured data, since rovibrational levels differ in fluorescence quantum yield and wavelengths. Consequently, the sensitivity of the method depends on the rovibrational distribution. The intensity of the measured fluorescence signal can be expressed as the sum of contributions from all spectral lines generated by the excited OH radical

$$M_f = \iiint_V \frac{\Omega}{4\pi} \int_0^\infty \sum_{v'v''} \sum_{J'J''} \sum_{\alpha'\alpha''} F\left(\lambda^{v'J'\alpha'}_{v''J''\alpha''}\right) D\left(\lambda^{v'J'\alpha'}_{v''J''\alpha''}\right) A^{v'J'\alpha'}_{v''J''\alpha''} N^{v'J'\alpha'} \,\mathrm{d}t\,\mathrm{d}V \tag{2}$$

with the following meaning of used symbols: Ω is the solid angle in which the fluorescence is collected by the detector, F is the transmittance of optics in front of the detector (usually the transmittance of an interference filter), D is the detector sensitivity, A is the emission coefficient for the particular line and N is the concentration of excited OH radical in the particular level described by vibrational number v', total orbital momentum number J' and doublet component α'. (The doublet component can have two values, usually labelled as 1 and 2.) λ is the wavelength of the particular line. The signal is integrated over the whole detection volume and the whole time of the detection process. The absolute detector sensitivity is usually not known and needs to be calibrated. However, the relative dependence of the sensitivity is simply achievable. Therefore, we will describe the detector sensitivity as a product $D = D_a \cdot d$ of a known function of wavelength $d(\lambda)$ and an unknown constant D_a.

Concentration of all excited levels involved in the fluorescence process can be calculated by means of a set of tens kinetic equations. Luckily, at atmospheric pressure the rotational equilibrium of each particular vibronic $A^2\Sigma^+$ state is often reached quickly, which can be used for a considerable simplification of the eq. (2). In this simplification, we will describe relative population of each rotational level by the Boltzmann factor

$$f_{v'J'\alpha'} = \frac{(2J'+1)\exp\left(-\frac{E_{v'J'\alpha'}}{kT}\right)}{\sum_{J'\alpha'}(2J'+1)\exp\left(-\frac{E_{v'J'\alpha'}}{kT}\right)} \tag{3}$$

and we will assume that saturation effects are negligible. At these assumptions the kinetic equations of the fluorescence process enable to express the fluorescence signal by

$$M_f = N_{Xi}\,\frac{\kappa B}{c}\,E_f\,\tau_1\left[\sum_{J'J''\alpha'\alpha''} F\left(\lambda^{v'=1\,J'\alpha'}_{v''=1\,J''\alpha''}\right) d\left(\lambda^{v'=1\,J'\alpha'}_{v''=1\,J''\alpha''}\right) A^{v'=1\,J'\alpha'}_{v''=1\,J''\alpha''}\, f_{v'=1\,J'\alpha'}(T) + \right.$$

$$\left. + V\tau_0 \sum_{J'J''\alpha'\alpha''} F\left(\lambda^{v'=0\,J'\alpha'}_{v''=0\,J''\alpha''}\right) d\left(\lambda^{v'=0\,J'\alpha'}_{v''=0\,J''\alpha''}\right) A^{v'=0\,J'\alpha'}_{v''=0\,J''\alpha''}\, f_{v'=0\,J'\alpha'}(T)\right] \times \tag{4}$$

$$\times \iiint_V D_a\,\frac{\Omega}{4\pi}\,s\,\mathrm{d}V. \tag{5}$$

for excitation to the $v'=1$ state and detection of $1-1$ and $0-0$ vibrational bands and by

$$M_f = N_{Xi}\,\frac{\kappa B}{c}\,E_f\,\tau_0\left[\sum_{J'J''\alpha'\alpha''} F\left(\lambda^{v'=0\,J'\alpha'}_{v''=0\,J''\alpha''}\right) d\left(\lambda^{v'=0\,J'\alpha'}_{v''=0\,J''\alpha''}\right) A^{v'=0\,J'\alpha'}_{v''=0\,J''\alpha''}\, f_{v'=0\,J'\alpha'}(T)\right] \times \tag{6}$$

$$\times \iiint_V D_a\,\frac{\Omega}{4\pi}\,s\,\mathrm{d}V. \tag{7}$$

for excitation to the $v'=0$ state. N_{Xi} denotes the concentration of OH radicals in the particular rotational level of the ground vibronic state $\mathrm{X}^2\Pi(v''=0)$ from which the excitation occurred, B is the Einstein coefficient for absorption of the particular excitation transition, c is the speed of light and κ is the overlap term of the absorption and laser line [7], E_f is the mean energy of laser pulses during the measurement of the fluorescence, τ is the life-time of the relevant vibronic state and V is the $\mathrm{A}^2\Sigma^+(v'=1) \to \mathrm{A}^2\Sigma^+(v'=0)$ VET rate constant. The spatial laser beam profile s is proportional to the area density of laser energy and it is normalized to one when integrated in the plane perpendicular to the laser beam direction, i.e. $\iint_S s\,\mathrm{d}S = 1$. The value of the integral $\iiint_V D_a\,\frac{\Omega}{4\pi}\,s\,\mathrm{d}V$ can be calibrated by means of Rayleigh scattering.

Equations (5) or (7) can be used for calculation of OH concentration in the ground state. Since N_{Xi} includes only OH radicals in one particular rotational level, it is necessary to calculate the concentration of all OH radicals in the ground vibronic state $\mathrm{X}^2\Pi(v''=0)$ by means of the Bolzmann factor

$$N_X = N_{Xi}/f_{Xi} = N_{Xi}\,\frac{2\sum_j (2J_j+1)\exp\left(-\frac{E_j}{kT}\right)}{(2J_i+1)\exp\left(-\frac{E_i}{kT}\right)}. \tag{8}$$

The factor 2 in the numerator is caused by the Λ-doubling.

Calibration

The unknown integral $\iiint_V D_a\,\frac{\Omega}{4\pi}\,s\,\mathrm{d}V$ in eq. (5) and (7) usually needs to be calibrated. The constant D_a could be measured by means of a calibrated light source, but this procedure requires an independent determination of the laser-plasma interaction volume and does not take into account that the detection sensitivity may depend on the incidence angle of fluorescence radiation on the detection unit. Consequently, it is advantageous to calibrate the whole integral $\iiint_V D_a\,\frac{\Omega}{4\pi}\,s\,\mathrm{d}V$ directly, which can be achieved by measurement of Rayleigh scattering [8, 9] on a gas at known pressure and temperature.

The intensity of signal measured by Rayleigh scattering experiment can be expressed as

$$M_r = \frac{\mathrm{d}\sigma_r}{\mathrm{d}\Omega}\,N_r\,\frac{E_r}{h\nu_r}\,d(\lambda_r)\iiint_V D_a\,\Omega\,s\,\mathrm{d}V + m_s E_r, \tag{9}$$

where $\mathrm{d}\sigma_r/\mathrm{d}\Omega$ is the differential cross section for Rayleigh scattering, N_r is the concentration of atoms or molecules of the used gas, E_r is the mean energy of laser pulses during the collection of the scattering signal. ν_r and λ_r are the frequency and wavelength of laser radiation, respectively. $m_s E_r$ is a parasitic signal caused by laser scattering on surrounding objects or eventual dust particles in the gas. When this parasitic signal is eliminated, the equation (9) enables to determine the value of the unknown integral.

Besides optimization of laser beam shape and discharge apparatus, there are two basic ways how to eliminate the parasitic signal. The first way can be used when the discharge apparatus can be placed into a vacuum chamber. Since Rayleigh scattering intensity depends on gas pressure whereas scattering on surrounding objects not, it is easy to determine the m_s value from the dependence of measured scattering signal (M_r) on pressure and subtract the parasitic signal from measured data.

However, in some experiments vacuum can not be used and Rayleigh scattering must be realized in a reactor that is open to ambient atmosphere. Besides laser scattering on reactor parts, dust particles may penetrate to the scattering volume and increase the parasitic signal. In this case it is possible to use the anisotropy of Rayleigh scattering: Rayleigh scattering does not emit light to the direction parallel with laser polarization. Since scattering on surrounding objects and eventual dust particles does not depend markedly on laser polarization, it is possible to determine the parasitic signal intensity as the signal detected when laser polarization is turned by 90°.

Especially when dust particles can penetrate to the scattering volume, it is desirable to use suitable statistical processing of measured data. If sufficient number of scattering measurements is realized, it is possible to exclude deviating values (e.g. that differ from the mean value by more than triple of sample standard deviation) and/or to calculate the mean value of scattering signals from points between the first and third quartile.

References

[1] Möhlmann G, Beenakker C and De Heer F 1976 *Chemical Physics* **13** 375–385

[2] Voráč J, Synek P, Procházka V and Hoder T 2017 *Journal of Physics D: Applied Physics* **50** 294002

[3] Herzberg G and Spinks J W T 1950 *Molecular Spectra and Molecular Structure: Diatomic molecules* (Van Nostrand, Princeton) ISBN 978-0894642685

[4] Lefebvre-Brion H and Field R W 2004 *The Spectra and Dynamics of Diatomic Molecules* (Elsevier Academic Press)

[5] Luque J and Crosley D 1999 Lifbase: Database and spectral simulation program (version 1.5) vol 99

[6] Voráč J, Obrusník A, Procházka V, Dvořák P and Talába M 2014 *Plasma Sources Science and Technology* **23** 025011

[7] Voráč J, Dvořák P, Prochazka V, Ehlbeck J and Reuter S 2013 *Plasma Sources Science and Technology* **22** 025016

[8] Miles R B, Lempert W R and Forkey J N 2001 *Measurement Science and Technology* **12** R33

[9] Bucholtz A 1995 *Applied Optics* **34** 2765–2773